Superior flame retardancy of cotton by synergetic effect of cellulose-derived nano-graphene oxide carbon dots and disulphide-containing polyamidoamines

Jenny Alongi [a], Paolo Ferruti [a], Amedea Manfredi [a], Federico Carosio [b], Zhaoxuan Feng [c], Minna Hakkarainen, [c,*] Elisabetta Ranucci [a,*]

[a] *Dipartimento di Chimica, Università degli Studi di Milano, via C. Golgi 19, 20133, Milano, Italy;*

[b] *Dipartimento di Scienza Applicata e Tecnologia, Politecnico di Torino, viale Teresa Michel 5, 15121, Alessandria, Italy;*

[c] *Department of Fibre and Polymer Technology, KTH Royal Institute of Technology, Teknikringen 56, 10044 Stockholm, Sweden.*

Corresponding Authors

[a,*] Elisabetta Ranucci

Tel./Fax: +39 0250314132. E-mail: elisabetta.ranucci@unimi.it

[c,*] Minna Hakkarainen

Tel./Fax: + +46 8 790 82 71. E-mail: minna@kth.se

ABSTRACT

Linear polyamidoamines containing disulphide groups (SS-PAAs) were prepared by polyaddition of *L*-cystine with 2,2-bisacrylamidoacetic acid (B-CYSS), *N,N′*-methylenebisacrylamide (M-CYSS) and 1,4-bisacryloylpiperazine (BP-CYSS). They were evaluated as flame retardants for cotton, alone or with cellulose-derived nano-graphene oxide (nGO) carbon dots, to assess whether, due to their potential as radical scavengers, the latter would improve the already good performance of SS-PAAs. In vertical flame spread tests (VFST), cotton treated with 1% nGO burned as quickly as cotton, whereas B-CYSS, M-CYSS and BP-CYSS extinguished the flame at add-ons ≥ 12, 16 and 20%, respectively. Probably, the gaseous products of SS-PAA thermal degradation quenched the radicals involved in oxidation. Cotton treated with 8, 12 and 15%, respectively, of B-CYSS, M-CYSS and BP-CYSS burned completely, but further addition of 1% nGO either inhibited ignition or shortly extinguished the flame, demonstrating synergism between the two components. Synergism was confirmed by assessing the synergism effectiveness parameter for the residual mass fraction (RMF) and by comparing the calculated and experimental TG curves in air for the cotton/SS-PAA-nGO systems. In cone calorimetry tests, the presence of nGO did not improve the already good performances of SS-PAAs, supporting the hypothesis that the action of both takes place in the gas phase.

Keywords: Disulphide-containing polyamidoamines; PAAs; Graphene oxide; Functional coatings; Intumescent flame retardants; Cotton.

1. Introduction

Linear polyamidoamines (PAAs) are bioinspired polymers discovered in the late 1960s and later years extensively studied.[1-3] They are prepared by Michael-type polyaddition of *prim*- or bis-*sec*-amines with bisacrylamides. The reaction is preferably carried out in water at room temperature with neither organic solvents, nor added catalysts, nor by-products. All PAAs necessarily bear *tert*-amine and amide functions in the main chain. However, the Michael-type addition reaction is remarkably specific and allows to adopt many functional amines as monomers, obtaining PAAs assembling different additional functions either in the main chain or as side substituents. In particular, the polyaddition of bisacrylamides with several natural α-amino acids was performed and led to a new family of bio-inspired PAA-related polymers named polyamidoamino acids (PAACs).[4-8] PAAs carrying functions typically present in intumescent flame retardant formulations can be obtained. Recently, in fact, many PAAs have shown potential as surface confined flame retardant agents (FR) for cotton.[9] The best ones extinguished the flame in horizontal flame spread tests (HFST) at 4-12% add-ons. However, none of them extinguished the flame in vertical flame spread tests (VFST) at add-ons as large as 35%. Keratin, the collective name of disulphide-containing animal proteins abundant in skin and hairs, is well-known for its flame retardant properties. This suggested that the introduction of disulphide groups in PAAs (SS-PAAs) could endow similar properties.[10] SS-PAAs had previously been evaluated as bio-reducible biomedical polymers.[11, 12] Subsequently, it was found that at moderate add-ons (12-20%) several SS-PAAs extinguished the flame not only in horizontal, but also in vertical flame spread tests, a performance seldom, if ever, reported for fully organic FR. The remarkably increased flame retardant potency of SS-PAAs was attributed to their ability to evolve,

as keratin, sulphur-containing thermal decomposition products quenching the radicals involved in oxidation.[13, 14]

Recently, graphene and micro- and nanosized graphene oxide (GO and nGO, respectively) are receiving considerable attention in several fields, including also flame retardancy.[15-18] Graphene oxide is the common name indicating the non-stoichiometric compounds prepared by oxidation of graphite. Polystyrene mixed in bulk with GO 45-500 μm in size modified with organofunctional silane gave very good results in HFST but performed poorly in VFST.[19] The effect of GO addition into polycarbonate (PC), acrylonitrile-butadiene-styrene and high-impact polystyrene on the flammability of the resulting nanocomposites was also investigated. It was reported that GO-PC composites demonstrated very fast self-extinguishing times in vertical open flame tests.[20] nGO introduced into a polymer matrix performed as FR better than layered aluminosilicate clays.[21] Possibly, this result was due to the nanosized dimensions of the GO particles employed, allowing better dispersion inside the polymer mass. GO was suggested to act as FR because of its property of intumescing on heating.[19] However, radical scavenging is a well-documented GO property;[22] therefore, it can be reasonably assumed that the FR activity of the GO was due, in addition to intumescence, to its ability to entrap the radicals that sustained the combustion process. This ability is considered to play a paramount role also in the FR performances of keratin[13] and SS-PAAs.[10] This led us to hypothesize that the addition of small amount of nGO could increase the flame retardant performances of PAAs and, especially, SS-PAAs. To verify this hypothesis, HFST and VFST were performed with SS-PAA treated cotton fabrics after the addition of minor amounts of nGO derived by carbonization of α-cellulose. For comparison purpose, the FR performances of the same amount of nGO without SS-PAAs were also assessed.

2. Experimental section

2.1 Materials

L-Cystine (CYSS, >98.0%), *N*,*N*′-methylenebisacrylamide (M, 99%), lithium hydroxide monohydrate ($LiOH.H_2O$, 98%), HCl (37% aqueous solution), H_2SO_4 (95-98%), HNO_3 (70%), α-cellulose (commercial grade containing 3% of pentose) and D_2O (99.9%) were purchased from Sigma-Aldrich and used as received. Aqueous solutions were prepared using HPLC water. 2,2-Bisacrylamidoacetic acid (B, 98%)[23] and 1,4-bisacryloylpiperazine (BP, 97%)[24] were synthesized as previously described. Cotton fabric (COT) having an area density of 200 gm^{-2} was purchased from Fratelli Ballesio S.r.l. (Torino, Italy).

2.2 Characterizations

The chemical structure of synthesized SS-PAAs was assessed by ^1H nuclear magnetic resonance (NMR), collecting spectra in D_2O at 25 °C using a Bruker Avance DPX-400 NMR spectrometer operating at 400.13 MHz. The thermal stability of SS-PAAs, nGO and treated fabrics was assessed by thermogravimetric analysis (TGA) in nitrogen and air from 50 to 800 °C upon 10 °C min^{-1} heating rate, using a TGA/DSC 2 Star® System produced by Mettler-Toledo and placing samples (5 mg for fabrics and 2 mg for powders) in open alumina pans, in either inert or oxidative atmosphere under 50 mL min^{-1} gas flow. The surface morphology of untreated and treated cotton fabrics was analysed by a LEO-1450 VP scanning electron microscope (SEM) operating at 15 mm working distance, under 5 kV beam voltage. Fabric pieces (5 x 5 mm^2) were fixed to conductive adhesive tapes and gold-metalized. SS-PAAs, nGO and treated fabrics were analysed by attenuated total reflectance (ATR) Fourier transform infrared spectroscopy (FT-IR). FT-IR/ATR spectra were recorded between 4000 and 600 cm^{-1} range (32 scans and 4 cm^{-1} resolution), at room temperature,

by a Perkin-Elmer Frontier FT-IR/FIR spectrophotometer, equipped with a diamond crystal having a penetration depth of 1.66 μm.

2.3 Synthesis of disulphide-containing polyamidoamines (SS-PAAs)

B-CYSS12 and BP-CYSS12 were essentially prepared as previously described. Briefly: B-CYSS. 2,2-Bisacrylamidoacetic acid (1.980 g; 10 mmol) and LiOH monohydrate (0.420 g; 10 mmol) were dissolved in water (4 mL). CYSS (2.430 g; 10 mmol) and LiOH monohydrate (0.840 g; 20 mmol) were added to the solution. The reaction mixture was homogenized by gently stirring for 1 h, and then maintained at 25 °C for three days with occasional stirring. It was then diluted to 50 mL with HPLC water and the pH adjusted to 4.5 with 37% HCl. The final product was retrieved by freeze-drying.

^{1}H NMR (D_2O, 400 MHz), δ (ppm): 2.52-2.90 (m, C**H**$_2$CONH); 3.25-3.48 (m, C**H**$_2$S, C**H**$_2$N); 3.90-4.10 (br s, C**H**CH_2S); 5.50-5.60 (br s, NHC**H**COOH); 5.70-5.75, 6.10-6.25 (m, C**H**=C**H**$_2$). $\overline{M}_n = 1200$ determined by ^{1}H NMR from the number of terminal groups.

BP-CYSS. 1,4-Bisacryloylpiperazine (1.942 g; 10 mmol) was dissolved in water (4 mL) and CYSS (2.400 g; 10 mmol) and LiOH monohydrate (0.840 g; 20 mmol) were added to the solution. The reaction mixture was homogenized by gently stirring for 1 h, and then maintained at 25 °C for three days with occasional stirring. After this time, it was diluted to 50 mL with water and the pH adjusted to 4.5 with 37% HCl. The final product was retrieved by freeze-drying.

^{1}H NMR (D_2O, 400 MHz), δ (ppm): 2.92-3.34 (m, C**H**$_2$CONH); 3.33-3.44 (m, CHC**H**$_2$S); 3.36-3.40 (m, CHC**H**$_2$NH); 3.47-3.61 (m, C**H**CH_2S); 4.00-4.05 (m, NHC**H**COOH).

$\overline{M}_n > 10000$

M-CYSS was synthesized by following the same procedure described for BP-CYSS and using the following amounts of reagents: M-CYSS: M (1.541 g; 10 mmol), CYSS (2.403 g; 10 mmol) and LiOH monohydrate (0.839 g; 20 mmol).

^{1}H NMR (D_2O, 400 MHz), δ (ppm): 2.43-2.52 (m, C**H**$_2$CONH); 2.78-3.00 (m, CH**C**H$_2$S and CHC**H**$_2$NH); 3.36-3.42 (m, NHC**H**COOH); 4.53-4.70 (m, NHC**H**$_2$NH).

$\overline{M}_n > 10000$

2.4 Synthesis of graphene oxide type carbon dots (nGO)

Nano-graphene oxide (nGO) type carbon dots were synthesized from α-cellulose by microwave-assisted hydrothermal process according to previously reported process.[25] Briefly, the hydrothermal carbonization of α-cellulose was done in a Milestone flexiWAVE microwave oven. α-cellulose (2 g) was put into a microwave vial together with H_2SO_4 (20 mL; 0.1 gmL^{-1}). The oven was heated to 200 °C over a 20 min time period and then kept at 200 °C for 2 h. Carbon spheres (CS) were separated by filtration, purified by washing with deionized water followed by drying in the vacuum oven at 25 °C for three days. CS were transferred into nitric acid (10:1, w/v) solution in a round-bottom flask and sonicated in a bath for 30 min. The solution was heated 60 min at 90 °C under magnetic stirring. Deionized water (150 mL) was added to stop the reaction. Vacuum distillation was applied to remove the aqueous solution and the brownish nGO was obtained after freeze-drying. Detailed synthesis and characterization were previously described.[25]

2.5 Impregnation of cotton fabrics

Cotton fabric samples of 20 x 50 mm^2 size were first impregnated two or three time with a 8 wt.-% aqueous SS-PAA solution (6 and 9 pHs for B-CYSS and BP-CYSS, and M-CYSS, respectively)

and then with a 1.0 wt.-% nGO solution. After each deposition, samples were dried for 2 min at 90 °C. The total dry solid add-ons on cotton fabrics (*Add-on*, wt.-%) were determined by weighing each sample before (W_i) and, after drying, (W_f) after impregnations, first with the PAA solution and then with the nGO solution. The add-ons were calculated according to the following equation (*Eq.* 1):

$$Add - on = \frac{W_f - W_i}{W_i} \times 100 \ (Eq. 1)$$

Strips of SS-PAA, nGO and SS-PAA-nGO treated cotton will be coded as COT/SS-PAA, COT/nGO and COT/SS-PAA-nGO, respectively.

2.6 Combustion tests

For cotton fabrics, combustion tests in horizontal and vertical configurations were carried out by applying a 20 ± 5 mm long methane flame for 3 s on the short side of 20 x 50 mm^2 specimens. In horizontal configuration, the sample was positioned in a metallic frame tilted by 45° along its longer axis and then burnt. In vertical configuration the methane flame was applied for 3 s on the centre of the short side of specimens. All specimens were conditioned to constant weight at 27 ± 1 °C at 70% relative humidity and tests were triplicated. Total combustion time (s) and rate (mm s^{-1}), and residual small fraction (RMF, wt.-%) were assessed.

The resistance to 35 kWm^{-2} irradiative heat flux of square fabric samples (100 x 100 mm^2) was investigated using oxygen consuming cone calorimeter (Fire Testing Technology). Measurements were carried out in horizontal configuration, following the procedure described elsewhere[26] optimising the ISO 5660 standard.[27] Parameters such as the time to ignition (TTI, s), total heat release (THR, MJ m^{-2}) and peak of heat release rate (PHRR, kW m^{-2}) were measured. Average

carbon monoxide [CO] and carbon dioxide [CO_2] yields (both expressed in kg kg^{-1}), and residual mass fraction (RMF, wt.-%) were assessed as well. In order to establish an efficiency ranking of the SS-PAAs under study, the fire performance index (FPI), that is, the TTI to PHRR ratio, was calculated: the higher the FPI, the more efficient was the flame retardant system.[28] Prior to combustion tests, all specimens were conditioned to constant weight at 23 ± 1 °C for 48 h at 50% relative humidity in a climatic chamber. The experiments were performed in triplicate for each sample calculating the experimental error.

3. Results and discussion

3.1 Synthesis of SS-PAAs

The SS-PAAs considered were prepared following the synthetic process reported in Scheme 1. They were obtained in a single step by the polyaddition of *L*-cystine with 2,2-bisacrylamidoacetic acid (B-CYSS), *N,N′*-methylenebisacrylamide (M-CYSS) and 1,4-bisacryloylpiperazine (BP-CYSS), according to typical Michael-type polyaddition conditions leading to PAAs, i.e., in water, at pH 9-10 and at room temperature.[1-3]

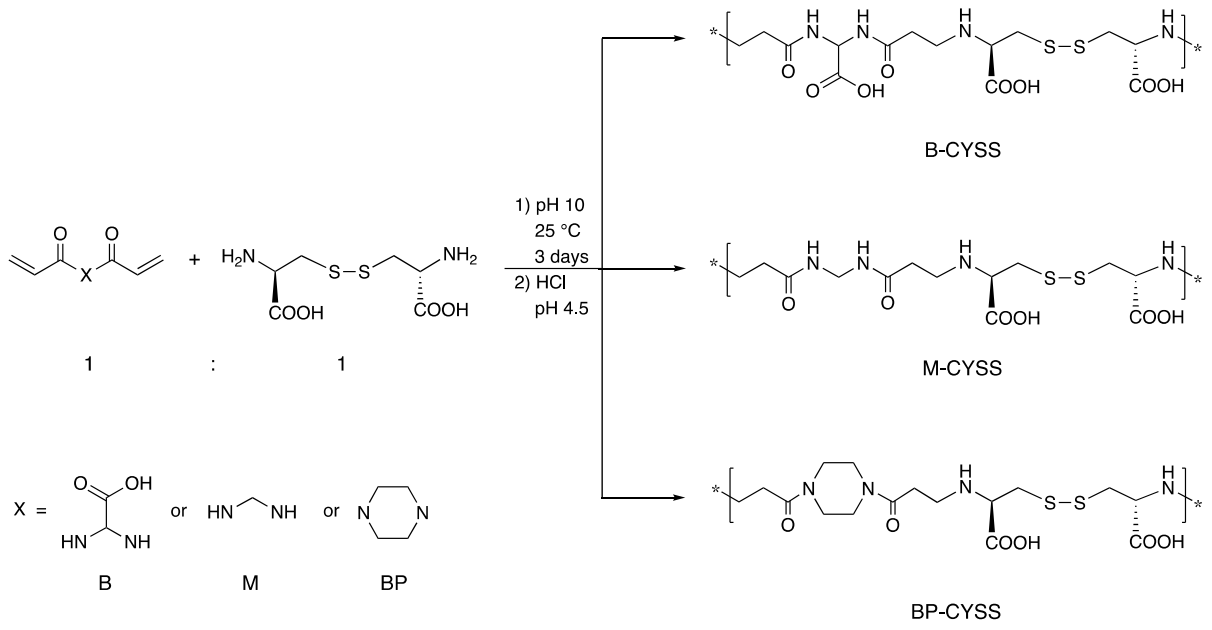

Scheme 1. Synthesis of SS-PAAs.

3.2 Thermal stability of SS-PAA

Figure 1 shows the TG thermograms of B-CYSS, M-CYSS and BP-CYSS carried out in both nitrogen and air in between 50-800 °C temperature range. $T_{onset10\%}$, onset decomposition temperature at 10% weight loss, T_{max}, temperature at maximum weight loss rate, and RMF, residual mass fraction measured at 750 °C, are reported in Table 2. As previously observed with sulphur-deprived PAAs studied as FR for cotton,[9] all SS-PAAs exhibited complex multimodal weight-loss curves in both nitrogen and air (Figure 1). For all SS-PAAs, the TG patterns in air were similar to those in nitrogen up to at least 400 °C. However, the values of both $T_{onset10\%}$ and T_{max1} in the series were rather different demonstrating that the type of bisacrylamide affected the thermal stability of SS-PAAs. The stability of all three PAAs was fairly high, as the RMF values found at 750 °C were 54-24% in nitrogen and 48-14% in air. In all cases, they were considerably higher than those of sulphur-deprived PAAs (29-7% in nitrogen versus 13-0% in air),[9] supporting the hypothesis that disulphide groups exerted a quenching effect on radical oxidation.[13] Among SS-PAAs, B-CYSS was the most thermally stable in both nitrogen and air. Based on $T_{onset10\%}$, T_{max1} and T_{max2} values, the relative thermal stability was B-CYSS > M-CYSS > BP-CYSS. As previously observed,[10] SS-PAAs showed lower weight loss in air than in nitrogen due to their intumescence in the 350-400 °C range (Figure 1). The relative thermal stability was B-CYSS > M-CYSS > BP-CYSS. In B-CYSS, the presence of an additional carboxyl group probably contributes to stabilization biasing the retro-Michael reaction by protonating the amine moiety of the repeat unit. Little difference is observed between the thermal stability of M-CYSS and BP-CYSS, the latter exhibiting a larger weight loss at T > 200 °C, possibly due to the lower concentration of SS groups deriving from the larger molecular mass of the repeat unit.

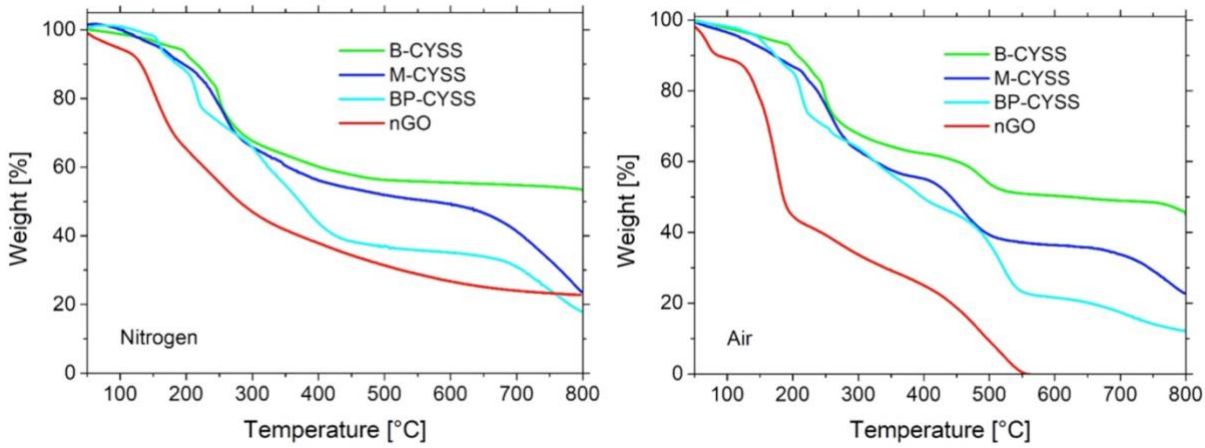

Figure 1. TG thermograms of SS-PAA and nGO in nitrogen and air.

Table 2. Thermal data of SS-PAA and nGO in nitrogen and air by thermogravimetric analysis.

SS-PAA	$T_{onset10\%}$ [a] [°C]	T_{max1} [b] [°C]	T_{max2} [c] [°C]	RMF at 750 °C [d] [%]
Nitrogen				
B-CYSS	216	200/230/**251**[e]	-	54
M-CYSS	195	174/**260**[e]	-	33
BP-CYSS	188	162/**216**[e]	-	24
nGO	131	150/**252**[e]	-	23
Air				
B-CYSS	207	200/228/**251**[e]	488	48
M-CYSS	171	221/228/**250**[e]	457	29
BP-CYSS	170	173/214/**258**[e]/**316**[e]	515	14
nGO	85	**176**[e]/270	480	0

[a] Onset decomposition temperature (temperature at 10% weight loss). [b] First temperature at maximum weight loss rate from dTG curves. [c] Second temperature at maximum weight loss rate from dTG curves. [d] Residual mass fraction at 750 °C. [e] Main decomposition event.

3.3 Thermal stability of nGO

The thermal stability of nGO alone was poor and it started losing weight already at low temperature. This was in agreement with previous studies, in which the early weight loss was due to the degradation and release of the oxygenated functional groups.[29] This was further supported by the increased thermal stability and decreased weight loss when nGO was reduced to decrease the number of oxygen functionalities.[30] The low thermal stability was also utilized for the production of reduced GO with lower degree of oxygenation by thermal treatment.[31]

3.4 Characterization of SS-PAA and nGO treated cotton fabrics

Cotton fabrics were first impregnated with SS-PAA aqueous solutions to different add-ons, then with an aqueous nGO suspension, and finally dried. In all cases, the nGO content was 1%. Table 3 lists the different compositions under investigation.

The SS-PAA flame retardants studied in this work are water soluble and if deposited as thin films on cotton fabrics are almost completely washed away with water after a few washing cycles. Chemically grafting SS-PAAs on cotton surface would obviously impart durability. In this regard, the Authors have already devised a synthetic strategy that, however, will be applied to previously optimized systems. Optimizing systems is precisely the aim of this paper. In this paper, in fact, the interaction of different SS-PAA/nGO systems with cotton, the understanding of the effect of the SS-PAA structure, of the SS-PAA/nGO ratio and of the deposition sequence on flame retardancy will be studied. Different behaviors of the SS-PAA/nGO systems will be identified provided that the add-ons of the FR components are precisely defined, and this condition can only be attained adopting the impregnation method.

Table 3. Cotton fabrics treated with SS-PAA, nGO and SS-PAA/nGO combination.

Sample	PAA-SS add-on [%]	nGO add-on [%]	Final add-on [%]
COT/B-CYSS_12	12.0	-	12.0
COT/M-CYSS_16	16.0	-	16.0
COT/BP-CYSS_20	20.0	-	20.0
COT/B-CYSS_8	8.0	-	8.0
COT/M-CYSS_12	12.0	-	12.0
COT/BP-CYSS_15	15.0	-	15.0
COT/nGO	-	1.0	1.0
COT/B-CYSS_8-nGO	8.0	1.0	9.0
COT/M-CYSS_12-nGO	12.0	1.0	13.0
COT/BP-CYSS_15-nGO	15.0	1.0	16.0

Fabrics were first characterized by FT-IR/ATR spectroscopy (Figure S1 in Supplementary Material). The FT-IR/ATR spectra of SS-PAA treated cotton revealed diagnostic bands ascribed to the three components, namely 3330 (ν O-H), 2925, 2850 (ν_{as} and ν_s CH_2), 1370 (δ C-H), 1310 (δ O-H), 1020 (ν C-O), and 894 cm^{-1} (ρ C-H) for cellulose, 1600 (ν C=O) and ~ 1520 cm^{-1} (δ N-H), less evident in the spectrum of treated cottons, as regards SS-PAAs (green, blue and azure asterisks in Figures S1 for B-CYSS, M-CYSS and BP-CYSS, respectively) and 1700 cm^{-1} (ν COOH) for nGO (red asterisks).

Figure 2 reports the SEM micrographs of untreated cotton, COT/B-CYSS_8, COT/nGO and COT/B-CYSS_8-nGO fabrics as an example of SS-PAA treated fabrics. The SEM micrographs of COT/M-CYSS_12, COT/ M-CYSS_12-nGO, COT/BP-CYSS_15 and COT/BP-CYSS_15-nGO are reported in Figures S2 and S3. After treatment with SS-PAAs or nGO, fibres maintained the natural spiralization and inhomogeneities of cellulose fibrils of cotton. In the presence of only SS-PAAs, the surface of fibres appeared smoother and the interstitial spaces were uniformly filled.

When cotton was treated with only nGO, a very thin coating covering the singular fibres was observed. SEM observations did not show particular differences in the morphology of cotton fibres when both SS-PAAs and nGO were deposited.

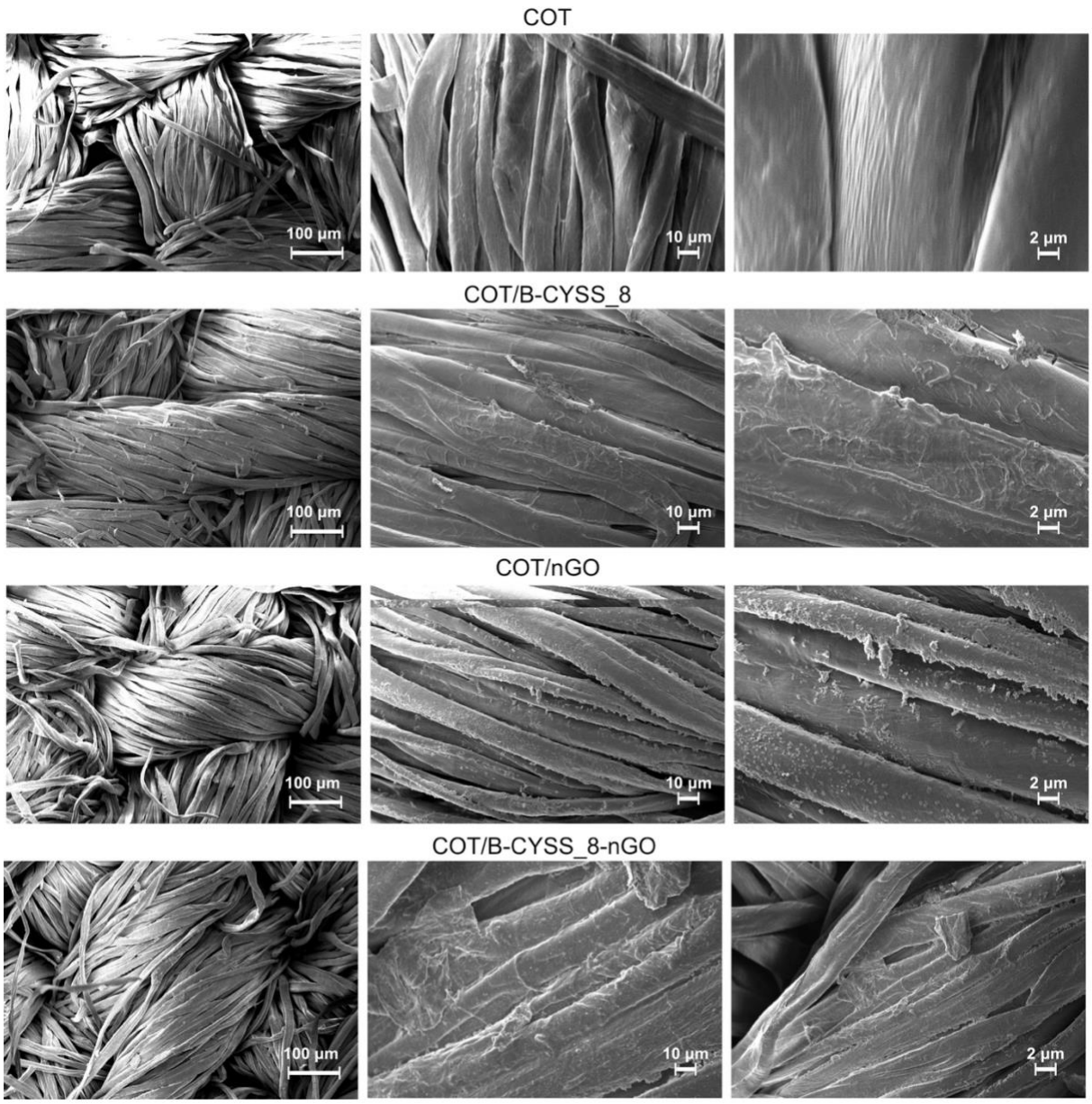

Figure 2. SEM micrographs of untreated-, B-CYSS (8% add-on), nGO (1% add-on) and B-CYSS_nGO (8+1% add-on) treated cotton fabrics.

3.5 Thermal stability of SS-PAA and nGO treated cotton

SS-PAA treated cotton started decomposing (Figure 3) at lower temperatures compared with untreated cotton (300-400 °C) in both nitrogen and air. The samples formed a higher amount of a thermally stable residue compared with untreated cotton (Table S1). In nitrogen, the residue remained almost constant by further heating, whereas it was oxidized in air. The presence of only nGO did not significantly change the thermal degradation of cotton (Figure 3).

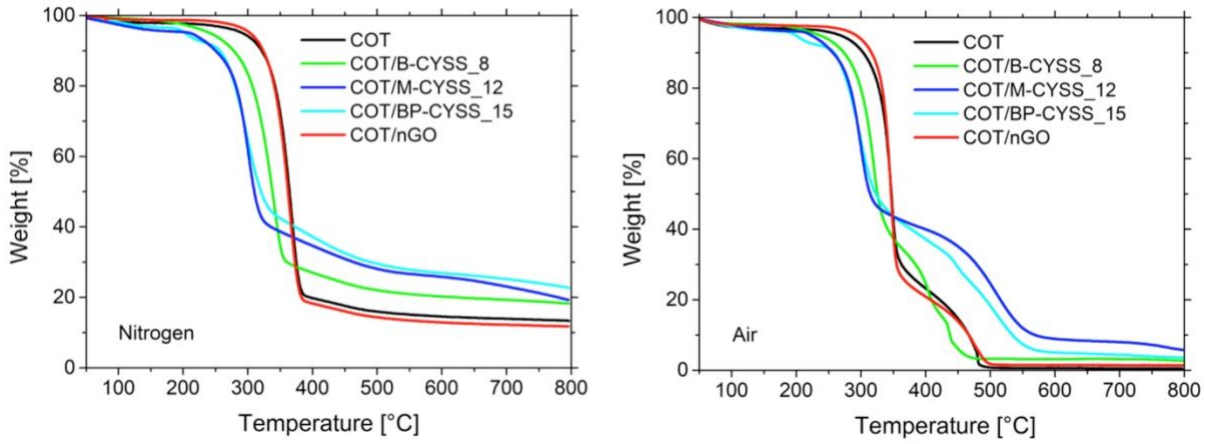

Figure 3. TG thermograms of SS-PAA and nGO treated cotton in nitrogen and air. Add-on values: COT/B-CYSS 8%, COT/M-CYSS 12%, COT/BP-CYSS 15%, and COT/nGO 1%.

Both in nitrogen and air, cotton treated with SS-PAA/nGO mixtures showed thermal pathways similar to those of SS-PAAs up to 350 °C (Figure 4). At higher temperatures, in the case of B-CYSS, in air, the char formed at 350 °C was slightly higher in the presence of nGO. Conversely, the residue left by M-CYSS and BP-CYSS was lower for nGO-based coatings with respect to those deprived ones.

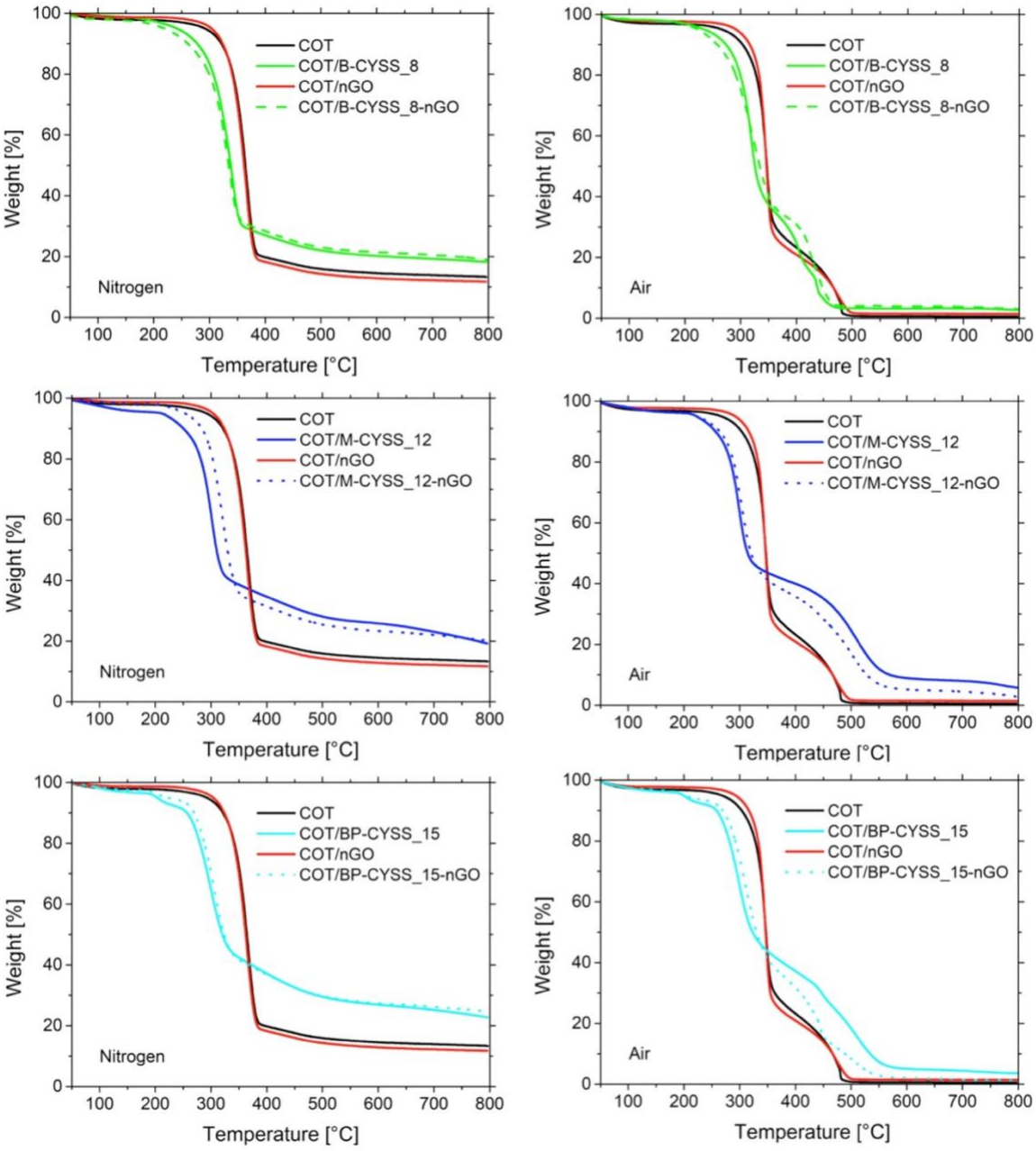

Figure 4. TG thermograms of SS-PAA-nGO treated cotton in nitrogen and air.

It may be noticed that above 350 °C the thermal degradation of COT/SS-PAAs-nGO is faster than that of COT/SS-PAAs. This might be explained as follows. It is well-known that nGO are effective radical scavengers.[22] On the other hand, the first step of the thermal decomposition of PAAs is the retro-Michael reaction, giving rise to unsaturated functions that on further heating evolve to

aromatic thermally stable structures responsible for char formation. This mechanism probably involved radicals. Therefore, the presence of nano-sized solid radical scavengers biases the formation of polycyclic aromatoid structures, and facilitated degradation on further heating. This phenomenon is less evident in the case of COT/B-CYSS-nGO because its add-on was considerably lower.

In order to investigate the synergism of the SS-PAAs/nGO combination on cotton flame retardancy, the experimental TG curves of the COT/SS-PAA/nGO systems were compared with the theoretical TG curves calculated by the additive calculation rule, according to *Eq*. 2:

$$W_{blend} = W_{COT}X_{COT} + W_{SS-PAA}X_{SS-PAA} + W_{nGO}X_{nGO} \quad (Eq.\ 2)$$

where W_{blend}, W_{cot}, $W_{SS\text{-}PAA}$ and W_{nGO} represent the weight of the blend and of the different components and X_{cot}, $X_{SS\text{-}PAA}$, and X_{nGO} the relative amounts of cotton, SS-PAA and nGO in the blend, respectively.

It can be observed (Figure 5) that in the range 200-320 ° C the experimental curves have moved towards significantly lower temperatures than those calculated, independently of the type of SS-PAA. On the contrary, in the range 320-420 ° C (320-530 °C in case of M-CYSS) the experimental curves have moved towards higher temperatures compared with the calculated ones. In fact, the theoretical and experimental curves are never overlapping, demonstrating that interactions between the components occurred. Consequently, the amount of char produced in the latter range of temperature was constantly higher, explaining the synergism in flame retardancy effectiveness.

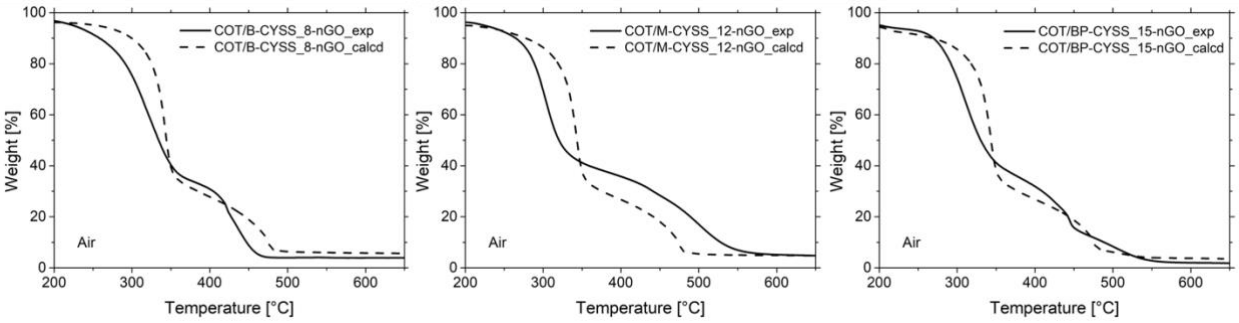

Figure 5. Comparison between experimental (coded as exp) and calculated (coded as calcd) TG thermograms of SS-PAA-nGO treated cotton fabrics in air. a): B-CYSS, b) M-CYSS and c) BP-CYSS.

3.6. Vertical flame spread tests

In VFST untreated cotton burned vigorously and completely, leaving no residue (Figure 6 and Table 4). In the same tests, B-CYSS, M-CYSS and BP-CYSS inhibited ignition at 12, 16 and 20% add-ons, only showing afterglow (Figure S4). At lower add-ons, 8, 12 and 15% for B-CYSS, M-CYSS and BP-CYSS, respectively, all samples burned, leaving a small residue (Figure 6 and Table 4). Cotton treated with 1% nGO completely burned as the untreated cotton.

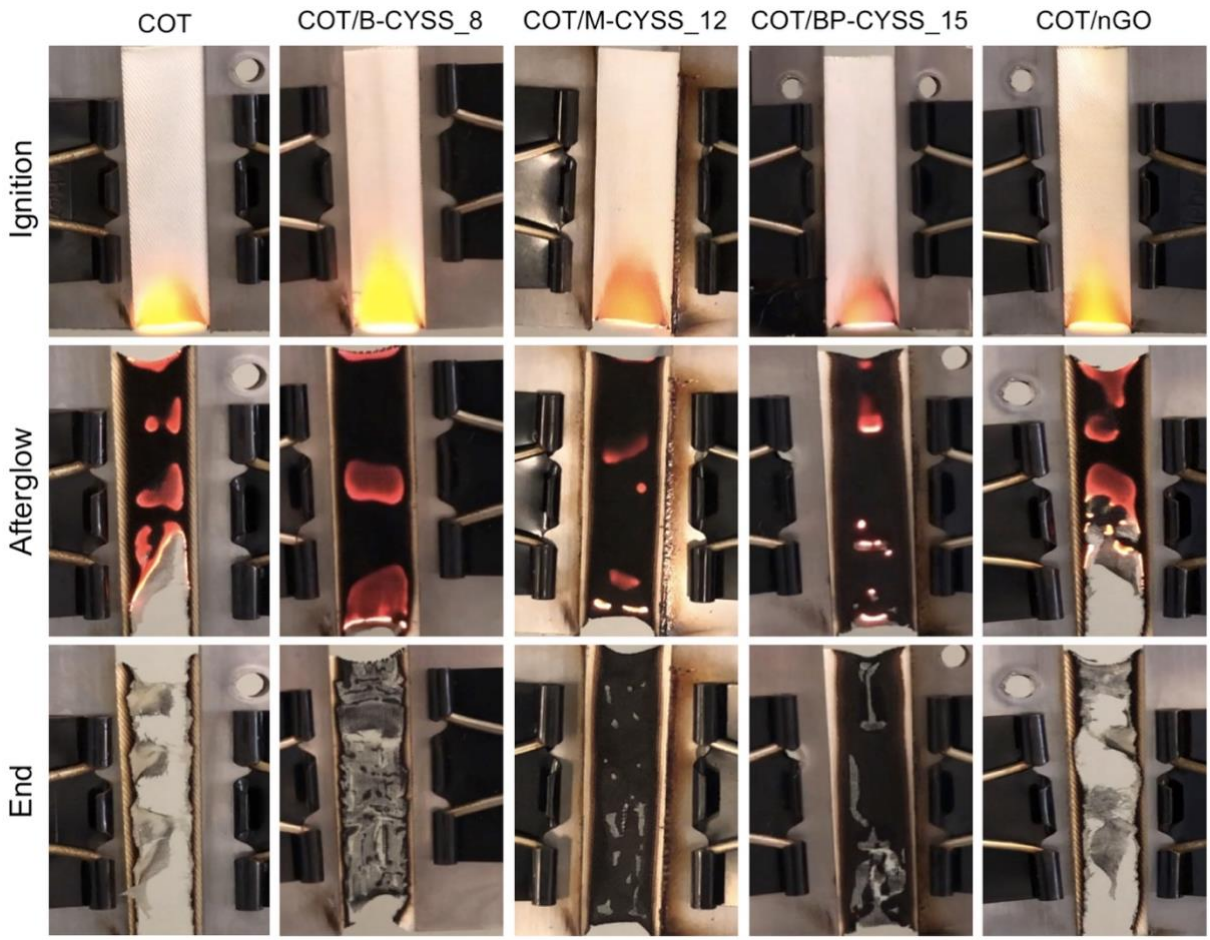

Figure 6. Snapshots of untreated, SS-PAA- and nGO treated cotton in vertical flame spread tests.

Table 4. Combustion data of SS-PAA- and SS-PAA-nGO treated cotton fabrics from vertical flame spread tests.

Sample	Notes	Total combustion		Extinguishment [YES/NO]	RMF_b [wt.-%]
		$time_a$ [s]	rate [mm s^{-1}]		
COT	Flaming	32	1.6	NO	1
COT/B-CYSS_12	No flaming, only afterglow	99	0.3	YES	72

COT/M-CYSS_16	No flaming, only afterglow	27	0.3	YES	87
COT/BP-CYSS_20	No flaming, only afterglow	28	0.2	YES	89
COT/B-CYSS_8	Flaming	60	0.8	NO	23
COT/M-CYSS_12	Flaming	90	0.6	NO	42
COT/BP-CYSS_15	Flaming	79	0.6	NO	43
COT/nGO	Flaming	29	1.7	NO	2
COT/B-CYSS_8-nGO	No flaming, only afterglow	10	0.8	YES	91
COT/M-CYSS_12-nGO	No flaming, only afterglow	15	0.3	YES	96
COT/BP-CYSS_15-nGO	No flaming, only afterglow	26	0.2	YES	93
SE B-CYSS-nGO	-	-	-	-	2.7
SE M-CYSS-nGO	-	-	-	-	2.3
SE BP-CYSS-nGO	-	-	-	-	2.1

[a] ±2 s; [b] ±1 wt.-%.

The addition of 1% add-on nGO reduced the minimal SS-PAA add-ons necessary to extinguish the flame down to 8, 12 and 15% for B-CYSS, M-CYSS and BP-CYSS, respectively, as demonstrated by the snapshots reported in Figure 7. Interestingly, these results were only obtained for samples in which nGO were added the last, after SS-PAA deposition.

In a previous work,[10] the FR effectiveness of SS-PAAs in VFST was ascribed to the thermal decomposition of the disulphide groups producing sulphur containing volatiles capable to quench the flame propagation in the gas phase. Most probably, these volatiles were thiyl radicals.[32] The

trend of the minimum add-ons required for flame extinguishment of cotton treated with the three SS-PAAs follows the trend of SS-PAA thermal stability, as shown in Figure 1 (see above).

The synergism between SS-PAAs and nGO can be explained considering the radical scavenging properties of nGO (see above).[22] The fact that, to be effective, nGO must be added the last, that is, as the top layer of the treated cotton, suggests that they work in the gas phase being drag by the evolving volatiles, thus enhancing their radical quenching ability in the gas phase.

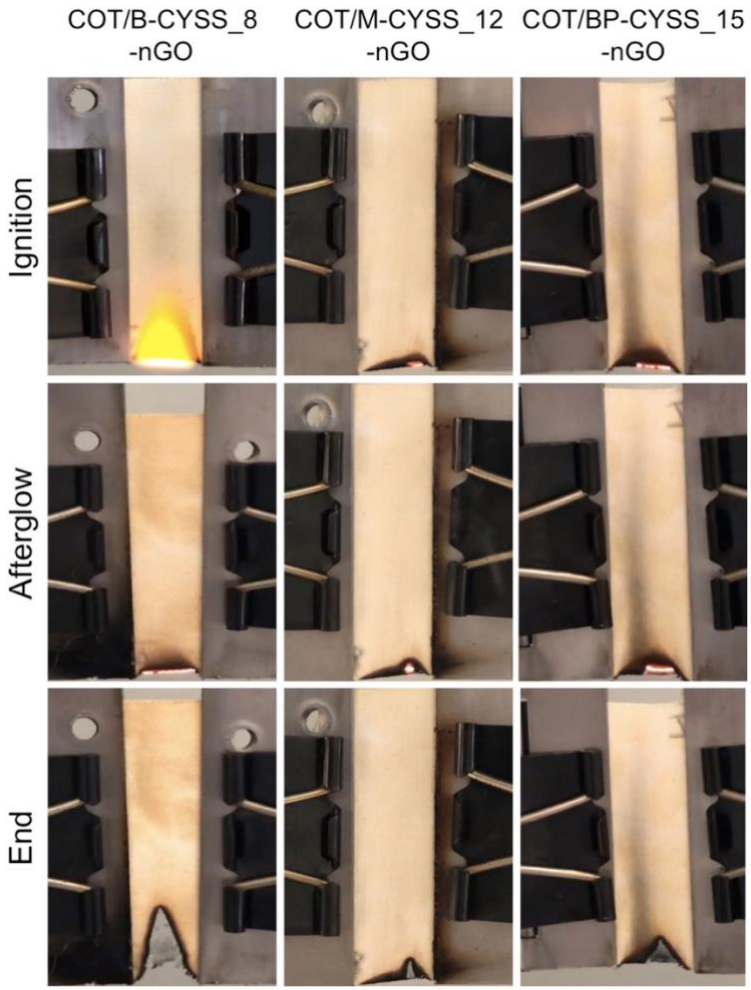

Figure 7. Snapshots of SS-PAA-nGO treated cotton in vertical flame spread tests. Add-on values: COT/B-CYSS-nGO 8+1%; COT/M-CYSS-nGO 12+1%; COT/BP-CYSS-nGO 15+1%.

As already discussed in the literature,[33, 34] synergistic effects between additives are defined to be superior to the superposition of the effects of each additive taken independently. In this work, in order to quantify the synergism between SS-PAAs and nGO, the *synergism effectiveness* (*SE*) parameter, described by Lewin[35-39], already applied for cotton fabrics\[40] and defined according to the following equation (*Eq*. 3), was calculated (Table 4):

$$SE = \frac{(Fp)_{fr+s} - (Fp)_p}{((Fp)_{fr} - (Fp)_p)) + ((Fp)_s - (Fp)_p))} \qquad (Eq.\ 3)$$

where (*Fp*) is a given flammability parameter (from flammability or combustion tests), $(Fp)_p$ is the flame-retardant property of the polymer alone (cotton), $(Fp)_{fr}$ is that of the polymer and flame retardant (cotton treated with SS-PAA), $(Fp)_s$ is that of the polymer treated with the synergist (cotton treated with nGO), and $(Fp)_{fr+s}$ is that of the full formulation comprising flame retardant and synergist (i.e. cotton treated with SS-PAA and nGO). In particular, $SE > 1$ means that synergy is occurring; $0 < SE \leq 1$ points out a simply additive effect; finally, $SE < 0$ implies antagonism.

The *SE* values were calculated only in case of RMF, because in case of combustion times and rates these values would be of little significance, since the COT/SS-PAA-nGO samples did not ignite. Consequently, only a minimal portion of the sample burned and the combustion time of this minimal portion was much lower than that of the untreated cotton, which burned completely. However, the RMF *SE* values were higher than 2, demonstrating the synergism existence.

3.7 Horizontal flame spread tests

In HFST, untreated and nGO treated cottons burned vigorously and completely, without leaving any residue (Figure 8 and Table 5). The synergism between SS-PAAs and nGO was observed in particular for B-CYSS. With 1% nGO, B-CYSS content was reduced from 12 to 8% add-on for

extinguishing flame. Moreover, cotton fabrics treated with 12 and 15% add-ons of M-CYSS and BP-CYSS, respectively, ignited cotton but soon extinguished the flame. After adding 1% nGO, they did not even ignite.

Figure 8. Snapshots of untreated, SS-PAA, nGO- and SS-PAA-nGO treated cotton in horizontal flame spread tests.

Table 5. Combustion data of SS-PAA- and SS-PAA-nGO treated cotton fabrics from horizontal flame spread tests.

Sample	Notes	Total combustion		Extinguishment [YES/NO]	RMF_b [wt.-%]
		$time_a$ [s]	rate [mm s^{-1}]		
COT	Flaming	52	1.0	NO	1
COT/B-CYSS_12	No flaming, afterglow	40	0.2	YES	93
COT/M-CYSS_16	No flaming, afterglow	7	0.3	YES	96
COT/BP-CYSS_20	No ignition	0	0	YES	99

COT/B-CYSS_8	Flaming	58	0.1	NO	27
COT/M-CYSS_12	Flaming	19	0.2	NO	91
COT/BP-CYSS_15	Flaming	35	0.1	NO	88
COT/nGO	Flaming	44	1.1	NO	1
COT/B-CYSS_8-nGO	No flaming, afterglow	19	0.2	YES	96
COT/M-CYSS_12-nGO	No ignition	8	0.3	YES	96
COT/BP-CYSS_15-nGO	No ignition	22	0.2	YES	95
SE B-CYSS-nGO		-	-	-	3.7
SE M-CYSS-nGO		-	-	-	1.1
SE BP-CYSS-nGO		-	-	-	1.1

[a] ±2 s; [b] ±1 wt.-%.

The RMF *SE* values were in all cases higher than 1, demonstrating the synergism existence.

3.8 Cone calorimetry tests

In order to simulate a realistic fire scenario, oxygen consumption cone calorimetry tests were performed by exposing cotton fabrics treated with SS-PAAs, nGO and SS-PAA/nGO to a 35 kWm^{-2} heat flux. This experimental condition is usually found in developing fires, capable of bringing the sample surface to approximately 520 °C.[28] Samples underwent thermo-oxidative degradation and released combustible volatile gases, leading to ignition of material and then combustion. Combustion parameters such as time to ignition (TTI), peak of heat release rate (PHRR), and total heat release (THR) are reported in Table 6. Figure 9 shows the heat release rate (HRR) curves of: a) COT/B-CYSS_8 and COT/B-CYSS_8-nGO, b) COT/M-CYSS and COT/M-CYSS_12-nGO, and c) COT/BP-CYSS_15 and COT/BP-CYSS_15-nGO, respectively. The HRR curve of COT treated with only 1 wt.-% nGO is not visible in Figure 9 since overlapped with that of untreated cotton. In agreement with the results of the flame spread tests, also the combustion parameters reported in Table 6 show that the presence of nGO did not affect cotton combustion.

On the other hand, all SS-PAAs reduced the PHRR value of cotton by 46, 52 and 50% for B-CYSS, M-CYSS and BP-CYSS, respectively. As previously observed[10] with different SS-PAAs, the TTI was not altered in the well-ventilated combustion scenario of cone calorimeter. Apparently, this is in contrast with the remarkable FR efficiency of SS-PAAs in VFST, but confirms the hypothesis that the action mode of both SS-PAAs and SS-PAA/nGO systems takes place in the gas phase, the former evolving sulphur volatiles quenching radicals, hence combustion, and nGO reinforcing the radical quenching activity by being drag in the gas phase owing to their nanometric dimensions. To this purpose, it should be reminded that the nGO action took place mainly when nGO were added on the top of the SS-PAA-treated cotton. Accordingly, the FPI values of SS-PAA-treated cotton were always higher than that of cotton, demonstrating their efficacy in flux irradiative combustion tests.[28] However, the addition of 1% nGO did not significantly change the FPI values. The same observation holds true for PHRR and RMF values.

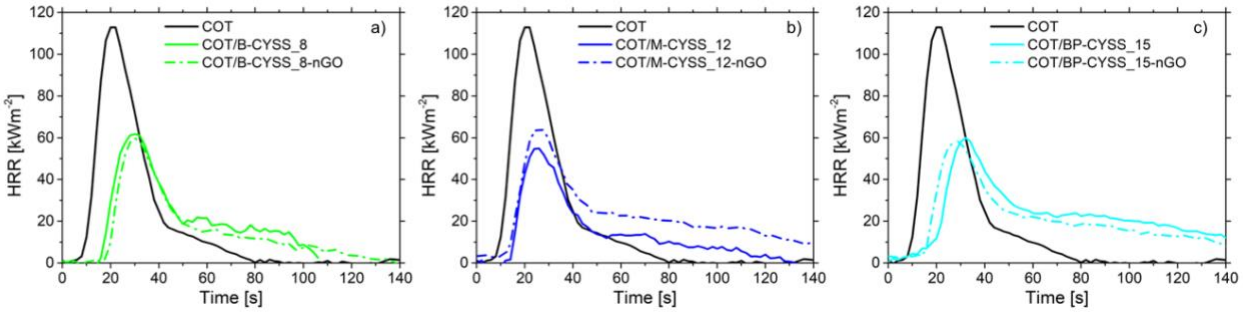

Figure 9. Heat release rate curves of: a) COT/B-CYSS_8 and COT/B-CYSS_8-nGO, b) COT/M-CYSS and COT/M-CYSS_12-nGO, and c) COT/BP-CYSS_15 and COT/BP-CYSS_15-nGO.

Table 6. Combustion data of cotton fabrics treated with SS-PAA and SS-PAA/nGO from cone calorimetry tests.

Sample	TTI[a] [s]	PHRR[b] [kWm-2]	ΔPHRR [%]	FPI[c] [sm2 kW-1]	THR[d] [MJm-2]	RMF[e] [wt.-%]
COT	12±4	116±6	-	0.10±0.05	2.2±0.1	-
COT/nGO	11±3	113±6	-	0.10±0.01	2.3±0.1	-

COT/B-CYSS_8	15±1	63±4	-46	0.24±0.01	2.1±0.1	5.5±0.5
COT/B-CYSS_8-nGO	16±1	65±3	-44	0.25±0.01	2.4±0.1	5.5±0.5
COT/M-CYSS_12	12±1	56±3	-52	0.22±0.01	2.2±0.1	5.0±0.5
COT/M-CYSS_12-nGO	14±1	54±3	-53	0.22±0.01	3.1±0.2	5.0±0.5
COT/BP-CYSS_15	19±1	58±3	-50	0.32±0.02	2.7±0.1	5.0±0.5
COT/BP-CYSS_15-nGO	18±1	60±3	-49	0.30±0.02	2.9±0.1	5.0±0.5

[a] Time To Ignition; [b] Peak of Heat Release Rate; [c] Fire Performance Index = TTI/PHRR; [d] Total Heat Release; [e] Residual Mass Fraction.

The release of [CO] and [CO_2] was monitored during combustion tests, and their average yield reported in Table 7. B-CYSS, M-CYSS or BP-CYSS significantly reduced both [CO] (by 51, 38 and 36%, respectively) and [CO_2] yields (by 19, 20 and 23%, respectively) of cotton. The addition of 1% nGO slightly increased [CO] and [CO_2] yields (2-3%), therefore seemingly reduces performance of SS-PAAs. This may be explained by the fact that nGO will ultimately burn producing both CO and CO_2.

Table 7. [CO] and [CO_2] yields of cotton fabrics treated with SS-PAA and SS-PAA/nGO from cone calorimetry tests.

Sample	[CO] [kg kg^{-1}]	Δ [CO] [%]	[CO_2] [kg kg^{-1}]	Δ [CO_2] [%]
COT	0.0650±0.0003	-	1.90±0.09	-
COT/nGO	0.0690±0.0004	-	2.04±0.10	-
COT/B-CYSS_8	0.0319±0.0016	-51	1.54±0.08	-19
COT/B-CYSS_8-nGO	0.0341±0.0017	-48	1.60±0.08	-16
COT/M-CYSS_12	0.0406±0.0020	-38	1.52±0.08	-20
COT/M-CYSS_12-nGO	0.0413±0.0021	-36	1.56±0.08	-18
COT/BP-CYSS_15	0.0471±0.0026	-28	1.46±0.07	-23

COT/BP-CYSS_15-nGO	0.0481±0.0024	-26	1.50±0.08	-21

4. Conclusions

The addition of 1% cellulose-derived nGO to SS-PAA treated cotton fabrics significantly reduced the minimum add-ons needed to extinguish the flame both in vertical and, albeit to a minor extent, in horizontal flame spread tests, whereas nGO alone was completely ineffective. The discovery of this significant synergism had great practical relevance, since it opened the way to a highly effective, non-toxic and environmentally friendly set of flame retardants for cotton and, possibly, for other ignitable materials.

Contrary to the results of VFST and HFST, the oxygen consumption cone calorimetry tests did not reveal any significant synergism between SS-PAA and nGO, suggesting that the synergism observed in VFST and HFST occurred in the gas phase. During the warm-up phase, the SS-PAAs developed volatile sulphur-containing compounds that not only extinguished the radicals involved in the combustion, but also dragged the nGO, known as radical scavengers, into the gas phase. In fact, nGO exerted their synergistic effect with FR with SS-PAAs only if they were added last to the cotton samples already treated with SS-PAAs. The ventilation in cone calorimetry tests obviously interfered with FR activities occurring in the gas phase.

As final consideration, the results obtained demonstrate that the research reported in this paper complies with most principles of green chemistry. In fact, the SS-PAA synthesis was performed in concentrated aqueous solution (30-40% w/w) and at room temperature without adding auxiliaries since the reaction is autocatalytic; moreover, it was a polyaddition and did not release by-products. One of the monomers was a natural amino acid, and the other a commercial product.

Both did not require previous derivatization. As for nGO, they were obtained by hydrothermal treatment of renewable sources with an effective microwave reaction.

Acknowledgments

The authors gratefully acknowledge the contribution by Dr. Serena Cappelli, SmartMatLab - Università degli Studi di Milano, for thermogravimetric analyses; Mrs. Giuseppina Iacono, Politecnico di Torino, for SEM analyses.

J.A. thanks the Transition Grant 2015/2017 - Horizon 2020, Linea 1A of the Università degli Studi di Milano for financial support.

References

[1] F. Danusso, P. Ferruti, Polymer 11 (1970) 88-113.

[2] P. Ferruti, Polyamidoamines: past, present and perspectives, J. Polym. Sci., Polym. Chem. 51 (2013) 2319-2353.

[3] E. Ranucci, A. Manfredi, Polyamidoamines: versatile bioactive polymers with potential for biotechnological applications, Chem. Afr. 2 (2019) 167-193.

[4] P. Ferruti, N. Mauro, L. Falciola, V. Pifferi, C. Bartoli, M. Gazzarri, F. Chiellini, E. Ranucci, E. Amphoteric, Prevailingly Cationic L-Arginine Polymers of Poly(amidoamino acid) Structure: Synthesis, Acid/Base Properties and Preliminary Cytocompatibility and Cell-Permeating Characterizations, Macromol. Biosci. 14 (2014) 390-400.

[5] A. Manfredi, N. Mauro, A. Terenzi, J. Alongi, F. Lazzari, F. Ganazzoli, G. Raffaini, E. Ranucci, P. Ferruti, Self-ordering secondary structure of D- and L-arginine-derived polyamidoamino acids, ACS Macro Lett. 6 (2017) 987-991.

[6] F. Lazzari, A. Manfredi, J. Alongi, R. Mendichi, F. Ganazzoli, G. Raffaini, P. Ferruti, E. Ranucci, Self-structuring in water of polyamidoamino acids with hydrophobic side chains deriving from natural α-amino acids, Polymers 10 (2018) 1261.

[7] F. Lazzari, A. Manfredi, J. Alongi, R. Mendichi, F. Ganazzoli, G. Raffaini, P. Ferruti, E. Ranucci, D-, L- and D,L-Tryptophan-Based Polyamidoamino Acids: pH-Dependent Structuring and Fluorescent Properties, Polymers 11 (2019) 543.

[8] E. Ranucci, P. Ferruti, E. Lattanzio, A. Manfredi, M. Rossi, P.R. Mussini, F. Chiellini, C. bartoli, Acid-Base Properties of Poly(amidoamine)s, J. Polym. Sci., Polym. Chem. 47 (2009) 6977-6991.

[9] A. Manfredi, F. Carosio, P. Ferruti, E. Ranucci, J. Alongi, Linear polyamidoamines as novel biocompatible phosphorus-free surface confined intumescent flame retardants for cotton fabrics, Polym. Degrad. Stabil. 151 (2018) 52-64.

[10] A. Manfredi, F. Carosio, P. Ferruti, J. Alongi, E. Ranucci, Disulfide-containing polyamidoamines with remarkable flame retardant activity for cotton fabrics, Polym. Degrad. Stabil. 156 (2018) 1-13.

[11] E. Emilitri, E Ranucci, P. Ferruti, New poly(amidoamine)s containing disulfide linkages in their main chain, J. Polym. Sci., Polym. Chem. 43 (2005) 1404-1416.

[12] E. Emilitri, P. Ferruti, R. Annunziata, E. Ranucci, M. Rossi, L. Falciola, P. Mussini, F. Chiellini, C. Bartoli, Novel amphoteric cystine-based poly(amidoamine)s responsive to redox stimuli, Macromolecules 40 (2007) 4785-4793.

[13] W. Pawelec, A. Holappa, T. Tirri, M. Aubert, H. Hoppe, R. Pfaendner, C.-E. Wilen, Disulfides effective radical generators for flame retardancy of polypropylene, Polym. Degrad. Stabil. 110 (2014) 447-456.

[14] R. Pfaendner. Flame Retardants for Polyethylene. In: M. A. Spalding and A.M. Chatterjee. (eds) Handbook of Industrial Polyethylene and Technology. Hoboken (USA): Wiley Publishing; 2018, pp. 921-934.

[15] G. Malucelli, The role of graphene in flame retardancy of polymeric materials: Recent advances, Current Graphene Science 2 (2018) 27-34.

[16] A. Kausar, Z. Anwar, B. Muhammad, Overview of non flammability characteristics of graphene and graphene oxide-based polymeric composites and essential flame retardancy techniques, Polymer-Plastics Technology and Engineering 56 (2017) 488-505.

[17] H. Li, Y. Du. G. Yang. G. Zhu, Y. Gao, W. Ding, Flame retardance of modified graphene to pure cotton fabric, J. Fire Sci. 36 (2017) 111-128.

[18] B. Sang, Z. W. Li, X.-H. Yu, Z. J. Zhang, Graphene-based Flame Retardants: a review, J. Mater. Sci. 51 (2016) 8271-8295.

[19] M. Kędzierski, P. Jankowski, G. Jaworska, A. Niska, Graphite oxide as an intumescent flame retardant for polystyrene, Polimery 57 (2012) 347-353.

[20] A.L. Higginbotham, J.R. Lomeda, A.B. Morgan, J.T. Tour, Graphite oxide flame-retardant polymer nanocomposites, ACS Appl. Mater. Interfaces 1 (2009) 2256-2261.

[21] J. Wang, Z. Han, Comparative Study of Nanoeffect on Fire Retardancy of Polymer - Graphite Oxide Nanocomposites. In: M. Le Bras (ed) Fire Retardancy of Polymers: New application of Mineral Fillers. Verlag: Springer, 2005, p. 161-167.

[22] Y. Qiu, Z. Wang, A.C.E. Owens, I. Kulaots, Y. Chen, A.B. Kanec, R.H. Hurt, Antioxidant chemistry of graphene-based materials and its role in oxidation protection technology, Nanoscale 6 (2014) 11744-11755.

[23] P. Ferruti, E. Ranucci, F. Trotta, E. Gianasi, E.G. Evagorou, M. Wasil, G. Wilson, R. Duncan, Synthesis, characterisation and antitumour activity of platinum (II) complexes of novel functionalised poly(amido amine)s, Macromol. Chem. Phys. 200 (1999) 1644-1654.

[24] P. Ferruti, Poly(amido-amine)s, Macromol. Synth. 9 (1985) 25-29.

[25] Z. Feng, K. Odelius, M. Hakkarainen, Tunable chitosan hydrogels for adsorption: property control by biobased modifiers, Carbohydr. Polym. 196 (2018) 135-145.

[26] J. Tata, J. Alongi, F. Carosio, A. Frache, Optimization of the procedure to burn textile fabrics by cone calorimeter: part I. Combustion behavior of polyester, Fire Mater. 35 (2011) 397-409.

[27] ISO5660, Reaction-to-fire tests - Heat release, smoke production and mass loss rate Heat release rate (cone calorimeter method) and smoke production rate (dynamic measurement), Genève, 2015.

[28] B. Schartel, M. Bartholomai, U. Knoll, Some comments on the main fire retardancy mechanisms in polymer nanocomposites, Polym. Adv. Technol. 17 (2006) 772-777.

[29] K.H. Adolfsson, S. Hassanzadeh, M. Hakkarainen, Valorization of cellulose and waste paper to graphene oxide quantum dots, RSC Adv. 5 (2015) 26550-26558.

[30] N.B. Erdal, K.H. Adolfsson, T. Pettersson, M. Hakkarainen, A green strategy to reduced nano-graphene oxide through microwave assisted transformation of cellulose, ACS Sustainable Chem. Eng. 6 (2018) 1246-1255.

[31] I. Jung, D.A. Dikin, R.D. Piner, R.S. Ruoff, Tunable electrical conductivity of individual graphene oxide sheets reduced at “low” temperatures, Nano Lett. 8 (2008) 4283-4287.

[32] A. Vandeputte, M.-F. Reyniers, B. Marin, Theoretical study of the thermal decomposition of dimethyl disulfide, J. Phys. Chem. A 14 (2010)10531-10549.

[33] B. Schartel, C. A. Wilkie, G. Camino, Flame retardant polymers - a guide on the use of: Part I scientific terms and methods, J. Fire Sci .34 (2016) 447-467.

[34] B. Schartel, C. A. Wilkie, G. Camino, Recommendations on the scientific approach to polymer flame retardancy: Part 2 - Concepts, J. Fire Sci. 35 (2017) 3-20.

[35] M. Lewin, Synergism and catalysis in flame retardancy of polymers, Polym. Adv. Technol. 12 (2001) 215-222.

[36] M. Lewin, Synergistic and catalytic effects in flame retardancy of polymeric materials-an overview, J. Fire Sci. 17 (1999) 3-19.

[37] E.D. Weil. Additivity, synergism and antagonism in flame retardancy. In: W. C. Kuryla and A. J. Papa (eds) Flame retardancy of polymeric materials. New York: Marcel Dekker, 1975, pp. 185-243.

[38] E.D. Weil. Synergists, adjuvants and antagonists in flame retardant systems. In: A. F. Grand and C. A. Wilkie (eds) Fire retardancy of polymeric materials. New York: Marcel Dekker, 2000, pp. 115-145.

[39] M. Lewin and E. D. Weil. Mechanisms and modes of action in flame retardancy of polymers. In: A. R. Horrocks and D. Price (eds) Fire retardant materials. Cambridge: Woodhead Publishing; 2001, pp. 31–68.

[40] J. Alongi, C. Colleoni, G. Rosace, G. Malucelli, Phosphorus- and nitrogen-doped silica coatings for enhancing the flame retardancy of cotton: Synergisms or additive effects?, Polym. Degrad. Stabil. 98 (2013) 579-589.